NEXRAD DOPPLER WEATHER RADAR NETWORK: POTENTIAL FOR AREAWIDE SURVEILLANCE OF PEST INSECT MIGRATIONS

J. K. Westbrook
Areawide Pest Mgmt. Res. Unit, USDA/ARS
College Station, TX
W. W. Wolf
USDA/ARS, retired
S. Allen
National Weather Service, USDC/NOAA
League City, TX
J. D. Ward
National Weather Service, USDC/NOAA
New Braunfels, TX

Abstract

Targets such as flying insects, birds, and bats obscure the measurement of radar reflectivity and doppler velocity by weather radars. This study was conducted to determine the relationship of the concentration and velocity of adult bollworms, *Helicoverpa zea* (Boddie), and other similar-size targets with the base reflectivity and doppler velocity measured by the NEXRAD network of WSR-88D doppler weather radars. Relationships between entomological radar data, pilot balloon wind profile data, and WSR-88D reflectivity and doppler velocity data were investigated in the Lower Rio Grande Valley near the WSR-88D at Brownsville, Texas, and near the WSR-88D at New Braunfels, Texas, in the spring and summer of 1995 and 1996. Clear-air radar reflectivity often exceeded 4 dBZ, the lower reflectivity threshold on the WSR-88D radar display for precipitation-tracking mode. WSR-88D reflectivity was significantly correlated with the aerial concentration of adult bollworm-size targets. Doppler velocity was significantly correlated with the radial component of wind velocity, but the target velocity contributed to a mean bias of as much as 2.7 m/s. These results indicate that information about the local population dynamics and identity of migratory nocturnal insects can increase the accuracy of reflectivity and velocity measurements by WSR-88D radars, and lead to the development of algorithms which estimate the migratory flux of bollworms and other nocturnal insects.

Introduction

Non-meteorological targets often produce substantial clear-air echos (i.e., noise) on weather radar displays (Battan 1973; Rogers and Brown 1997). Such targets may increase atmospheric reflectivity and returned radar power in a manner similar to that caused by precipitation. In addition to confounding the reflectivity pattern, insects, birds, bats and other flying organisms can also alter the radial velocities measured by doppler weather radars and wind profilers (Larkin 1991; Jain et al. 1993; Miller et al. 1996).

A national network (NEXRAD) of S-band (10-cm wavelength) WSR-88D doppler weather radars was started in 1990 (Crum and Alberty 1993). The WSR-88D radars are located throughout the contiguous U.S. and provide nearly complete coverage at an altitude of 3048 m above site level. Radar measurements include reflectivity, doppler velocity, and spectrum width (a measure of velocity variance), which are measured to a maximum range of 460 km, 230 km, and 230 km, respectively. The radar completes a volume scan of azimuthal sweeps at several elevation angles every 6 minutes in precipitation-tracking mode, and every 10 minutes in clear-air mode. Reflectivity algorithms are based on the assumption that the range volume of the radar beam is filled with spherical water droplets of known radius, and that the droplet radius is less than 1/10 of the radar wavelength to satisfy the Rayleigh law for the scattering of electromagnetic radiation by the droplets. Comprehensive descriptions have been written for WSR-88D data products (Klazura and Imy 1993) and doppler radar theory (Doviak and Zrnic 1984; NOAA 1990).

X-band (3-cm) radars have been used in entomological studies for several decades (Reynolds 1988). Radar entomological measurements have been especially useful in detecting high-altitude nocturnal flight of insects (Wolf et al. 1995). The nightly and seasonal periodicity of insect flight has also been determined by radars (Beerwinkle et al. 1993). Wolf et al. (1993) measured radar cross-sections of bollworm moths and other insects in the laboratory to determine the potential of classifying radar-detected insect targets based on body length and width. Smith and Riley (1996) developed a vertical-looking radar system which classifies aerobiological targets based on body length, body width, target speed, mass, and wing beat frequency.

The timing and concentration of adult bollworm emergence depends largely on the plant species, abundance, and phenological stage of host plants. Raulston et al. (1992) excavated insect pupae and determined that one to seven billion adult bollworms emerged annually from the generation produced on $2x10^5$ ha of fruiting corn in the Lower Rio Grande Valley (LRGV) of northeastern Mexico and southern Texas. Wolf et al. (1995) found that airborne concentrations of insects detected by radar compared well with the estimated emergence and airborne flux of adult bollworm (moths) from fields of host crops. Bollworm moth flight typically begins at about 0.5 hours after sunset; peaks at about one hour after sunset; and then declines steadily until ending about 0.5 hours before sunrise (Wolf et al. 1986). Bollworms and many other noctuid species are typically distributed within the lowest 1 to 2 km of the troposphere, and may congregate within concentrated layers and orient toward a collective heading (Wolf et al. 1995).

Reprinted from the *Proceedings of the Beltwide Cotton Conference*
Volume 2:1304-1310 (1998)
National Cotton Council, Memphis TN

A study was conducted to quantify the effects of night-flying insects on WSR-88D clear-air mode base reflectivity and base velocity measurements during periods of peak emergence and emigration of bollworm moths from cultivated habitats. The objectives of this research were: (1) to determine the effect of airborne insect concentration on WSR-88D radar reflectivity values; and (2) to determine the effect of insect flight on WSR-88D radial velocity values.

Methods

Site Description

Native vegetation in the LRGV is mostly comprised of mesquite, chapparal, prickly pear cactus, and bunch grasses, but irrigation has allowed more than 1/3 of the LRGV to be cultivated for the production of corn, cotton, sorgum, citrus, and other fruit and vegetable crops (Orton et al. 1967). Corn was grown on about 200,000 ha of irrigated land in the LRGV in 1995, but a severe drought reduced the corn production area by about 90% in 1996. The Gulf of Mexico forms the eastern border of the LRGV.

New Braunfels is surrounded to the east by field crops (especially corn) and pastures, and to the west by rocky terrain of the Balcones Escarpment (Texas Hill Country). Large populations of Mexican free-tail bats, *Tadarida brasiliensis*, occupy Bracken Cave and other caves in the Texas Hill Country. Mexican free-tail bats migrate annually to the Texas Hill Country and consume large quantities of night-flying insects including bollworms and other noctuids.

WSR-88D Doppler Radar Measurements

Level II data tapes for WSR-88D radar facilities at Brownsville (KBRO) and New Braunfels (KEWX), Texas, were acquired for analysis of doppler weather radar data products. The level II data tapes were loaded on an Exabyte 8500 5GB SCSI 8-mm tape drive and processed on either a Sun Ultra 1/170 Creator 3D with 128MB RAM and 25.2GB Storage Array running Solaris 2.51, or on a Sun Sparcstation 10/40 with 64MB RAM and a 4GB Seagate hard disk running Solaris 2.5. IRAS-Motif software (Priegnitz, 1995) was run to create base images of reflectivity and velocity for specific elevation scans, and to compute mean and maximum values for several specified areas (~10 km^2) within the surveillance regions (Table 1).

Entomological Radar Measurements

Several X-band (3-cm wavelength) radars were operated near two WSR-88D installations at Brownsville (KBRO), Texas, and New Braunfels (KEWX), Texas. Figs. 1 and 2 show the relative location of the field sites near Brownsville and New Braunfels, respectively. The X-band radars could detect individual bollworm moth-size targets to a maximum range of 2.2 km. Two scanning entomological radars (GBR-1 and GBR-2) were operated near New Braunfels and Hebbronville, Texas, in 1995 and 1996, and near Donna, Texas, in 1996. Aerial concentrations of bollworm moth-size targets were estimated by counting the number of targets within an annulus on the plan position indicator (ppi) display and dividing by the detection volume within the annulus. One ground-based scanning radar (GBR-1) used a counting annulus from 0.80 to 0.96 km range for eleven elevation scans from 3° to 72°. A second ground-based scanning radar (GBR-2) used a counting annulus from 1.21 to 1.40 km for eight elevation scans from 4° to 65°. Concentration data from GBR-2 were linearly interpolated to 100-m above ground level (AGL) intervals for analysis. An automatic vertical-pointed radar (VPR) (Beerwinkle et al. 1993) was operated in June 1995 and March 1996 at Moore Air Base near Edinburg, Texas, and near New Braunfels in August 1996. The VPR generated insect flux values every five minutes at vertical intervals of 39 m from the surface to 1.8 km AGL. Additional radar specifications are presented in Table 2.

Rawinsonde and Pilot Balloon Measurements

Vertical profiles of wind velocity were measured by tracking pilot balloons using one of three methods: optical theodolite, optical theodolite with a radiosonde receiver, or scanning radar. Azimuth angles and elevation angles were smoothed by an 11-point, centered, moving average scheme. Three-dimensional trajectories of the pilot balloons were calculated from the smoothed azimuth and elevation angles. Wind velocity values were calculated as the time rate of change of the individual horizontal coordinates. Values of wind velocity nearest to 50-m AGL intervals were output for subsequent statistical analysis.

Statistical Analysis

Mean and maximum WSR-88D reflectivity values within specified areas from the 0.5° elevation scan were output at 10-minute intervals and rounded to the nearest 10 mins. GBR-1 and GBR-2 provided insect concentration values (i.e., number of targets per volume), and the VPR measured the number of targets per volume per time. Observation times for values of insect concentration from GBR-1 and GBR-2 were rounded to the nearest half-hour and retained for analysis if coincident with WSR-88D scan times. Observation times for values of insect flux from the VPR were rounded to the nearest 5 mins. and retained for analysis if coincident with WSR-88D scan times. VPR data in the lowest four altitude intervals were excluded from analysis. The VPR insect count data were divided by the product of the range interval volume (38.1 m), beam radius, sampling duration (300 secs.), and wind speed to derive insect concentrations. Reflectivity values were regressed with values of insect concentration estimated for the altitude of the WSR-88D beam centerline and averaged throughout the beam width using PROC REG of the SAS version 6.12 statistical software (SAS Institute 1992). Regression values were tested for significance using critical values of the Pearson correlation coefficient.

Mean and maximum WSR-88D doppler velocity values within specified areas from the 0.5° elevation scan were output at 10-minute intervals. Observation times for values of wind velocity were rounded to the nearest half-hour, and records were retained for analysis if coincident with WSR-88D scan times. Mean bias and root-mean-square errors were calculated for the difference between values of the mean doppler velocity and the radial component of wind velocity. Values of doppler velocity were regressed with the radial component of wind velocity using PROC REG of the SAS version 6.12 statistical software (SAS Institute 1992). Regression values were tested for significance using critical values of the Pearson correlation coefficient.

Results and Discussion

The aerial abundance of insects in the LRGV in June 1995 appeared to be well represented by reflectivity maps. For example, the Brownsville WSR-88D often detected a cluster of maximum reflectivity which originated over the irrigated crop production area in the LRGV about 0.5 h after sunset (2100 h local time or 0200 Universal Coordinated Time [UTC]), and displaced downwind toward the northwest (Figure 3). The temporal pattern of mean reflectivity in the LRGV in June 1995 matched the pattern of aerial insect concentration during peak emergence of bollworms from fruiting corn per previous entomological radar investigations: (1) mean reflectivity increased rapidly from sunset to about 1 h after sunset, then decreased monotonically until sunrise (Figure 4); and (2) mean reflectivity decreased monotonically from 2 June to 11 June which corresponded with the second half of the estimated two-week (sigmoidal) bollworm emergence cycle (Figure 5). Entomological (X-band) radar measurements were unavailable during June 1995.

A summary of the regression between reflectivity and insect concentration is presented in Table 3. Insect concentration explained between 20% and 89% of the variance of radar reflectivity (significant at $\alpha = 0.05$). The value of r^2 was least in June 1996 when the X-band radar (GBR-2) was more than three times farther from the nearest WSR-88D than in July 1995 and August 1996. The standard error of estimate (S.E.) for mean reflectivity ranged from 2.78 to 6.45 dBZ. Figure 6 shows a scatter plot representation of the regression between reflectivity and insect concentration using GBR-2 in August 1996.

Results of the regression between doppler velocity and the radial component of wind velocity are summarized in Table 4. Wind velocity explained between 53% and 72% of the variance of doppler velocity (significant at $\alpha = 0.05$). The value of r^2 was greater for the mean radial component of wind velocity than for the centerline value of the radial component of wind velocity. Doppler velocity exceeded the radial component of wind velocity by a mean bias of 0.5 to 2.7 m/s. The mean bias was minimum in August 1996 when the wind was highly variable, and maximum in June 1996 when the wind was persistently from the southeast and bollworms were probably collectively aligned toward the north. The root-mean-square error (RMSE) for estimating doppler velocity ranged from 1.7 to 3.1 m/s. The bias and RMSE values are reasonable for bollworm flight which averages 4.5 m/s. Further, bias and RMSE values should be maximum when the radar beam radial is aligned with a collective insect flight heading, and minimum when the radial is perpendicular to the collective heading. Figure 7 shows a scatter plot representation of the regression between doppler velocity and the radial component of wind velocity in August 1996.

Conclusions

WSR-88D doppler weather radars show good potential to estimate the aerial concentration and displacement of night-flying insects during peak migrations. Significant relationships between reflectivity and insect concentration were documented between ranges of 15 to 69 km from the nearest WSR-88D, and clear-air reflectivity maps indicated that the coverage may extend beyond 180 km during peak migrations. Larger values of insect concentration should be obtained for regression with reflectivity to develop more robust relationships.

Doppler velocity was significantly correlated with the radial component of wind velocity, and we attributed bias estimates of speed to collective insect flight heading. Caution must be exercised in interpreting radar-estimated wind speed values because bollworm moths can contribute 4.5 m/s to the radar-estimated wind speed. For example, weather forecasters often rely on the radar velocity measurements to detect low-level wind jets, wind shear, advection, and other wind profile features.

Wind speeds estimated from the annulus of WSR-88D doppler velocity values at constant altitudes may be used to advect reflectivity values and estimate areawide insect dispersal for crop protection advisories. More field measurements of atmospheric refractive index, wind velocity, and the identity, vertical distribution, aerial concentration, and flight behavior of insect species are needed to improve the agriculturally-useful information which can be derived from WSR-88D data products.

Acknowledgments

P.D. Lingren initiated the collaboration between insect migration scientists and operational meteorologists for developing insect monitoring applications of the NEXRAD WSR-88D doppler weather radar system. J.A. Lee and S. Fuller were fully responsible for installing software, processing data, and generating graphics. R.S. Eyster, P.G. Schleider, E.C. Lawrence, A.A. Morrison, and J.A. Lee assisted with the meteorological and radar entomological field operations. D. Priegnitz and R. Johnson responded to our questions about the proper use of IRAS-Motif software modules. R. Lacey permitted our use of Sun workstations and peripherals for processing the Level II data tapes. T. Crum provided the WSR-88D Level II data tapes which

were used for the field operations in May and June 1995. N. Rydell, P. Yura, J. Snyder, and B. Read were especially helpful in ensuring the requested scanning mode and archiving of WSR-88D data products during the field operations.

References

Battan, L.J. 1973. Radar Observation of the Atmosphere. Univ. of Chicago Press. Chicago, IL. 324 pp.

Beerwinkle, K.R., J.A. Witz, and P.G. Schleider. 1993. An automated, vertical looking, X-band radar system for continuously monitoring aerial insect activity. Trans. Amer. Soc. Agric. Engrs. 36: 965-970.

Crum, T.D., and R.L. Alberty. 1993. The WSR-88D and the WSR-88D Operational Support Facility. Bull. Amer. Meteor. Soc. 74, 1669-1687.

Doviak, R. J. and D. S. Zrnic. 1984. Doppler Weather Radar and Weather Observations. Academic Press. London, UK. 458 pp.

Klazura, G. E. and D. A. Imy. 1993. A description of the initial set of analysis products available from the NEXRAD WSR-88D system. Bull. Amer. Meteor. Soc. 74, 1293-1311.

Jain, M., M. Eilts, and K. Hondl. 1993. Observed differences of the horizontal wind derived from doppler radar and a balloon-borne atmospheric sounding system. 8th Symp. on Meteorol. Observations and Instrumenation, Anaheim, CA, Jan. 1993, Amer. Meteorol. Soc., Boston, MA.

Larkin, R. P. 1991. Sensitivity of NEXRAD algorithms to echoes from birds and insects. 25th Intl. Conf. on Radar Meteorology, Paris, France. Amer. Meteorol. Soc., Boston, MA., 203-205.

Miller, P. A., M. F. Barth, J. Smart, and L. Benjamin. 1996. Bird contamination in the NOAA Profiler network hourly winds: results before and after implementation of the new quality control check. FSL Forum (Dec. 1996): 10-17, NOAA Forecast Systems Laboratory, Boulder, CO.

NOAA. 1990. Doppler radar meteorological observations; Part B: Doppler radar theory and meteorology (Interim Version One). U.S. Dept. of Commerce, Natl. Oceanic and Atmos. Admin., Washington, DC. Fed. Meteorol. Handbook No. 11.

Orton, R., D. J. Haddock, E. G. Bice, and A. C. Webb. 1967. Climatic Guide: the Lower Rio Grande Valley of Texas. Texas Agricultural Experiment Station, Bulletin No. MP-841. 108 pp.

Priegnitz, D. L., 1995: IRAS: software to display and analyze WSR-88D radar data. 11th Intl. Conf. on Interactive Information and Processing Systems for Meteorology, Oceanography, and Hydrology, Amer. Meteorol. Soc., Boston, MA., 197-199.

Raulston, J. R., S. D. Pair, J. Loera, A. N. Sparks, W. W. Wolf, J. K. Westbrook, G. P. Fitt, and C. E. Rogers. 1992. Helicoverpa zea (Lepidoptera: Noctuidae) pupa production in fruiting corn in northeast Mexico and south Texas. Environ. Entomol. 21: 1393-1397.

Reynolds, D. R. 1988. Twenty years of radar entomology. Antenna 12: 44-49.

Rogers, R. R. and W. O. J. Brown. 1997. Radar observations of a major industrial fire. Bull. Amer. Meteorol. Soc. 78: 803-814

SAS Institute. 1992. SAS/STAT User's Guide, Release 6.08. SAS Institute, Cary, NC.

Smith, A .D. and J. R. Riley. 1996. Signal processing in a novel radar system for monitoring insect migration. Computers and Electronics in Agric. 15, 267-278.

Wolf, W. W., J. K. Westbrook, and A. N. Sparks. 1986. Relationship between radar entomological measurements and atmospheric structure in south Texas during March and April 1982. In Sparks, A.N. (ed.), Long-range Migration of Moths of Agronomic Importance to the United States and Canada: Specific Examples of Occurrence and Synoptic Weather Patterns Conducive to Migration. U.S. Dept. of Agriculture. Washington, D.C. Report ARS-43, 84-97.

Wolf, W. W., C. R. Vaughn, R. Harris, and G. M. Loper. 1993. Insect radar cross-sections for aerial density measurements and target classification. Trans. Amer. Soc. Agric. Engrs. 36: 949-954.

Wolf, W. W., J. K. Westbrook, J. R. Raulston, S. D. Pair, and P. D. Lingren. 1995. Radar observations of orientation of noctuids migrating from corn fields in the Lower Rio Grande Valley. Southwestern Entomol. Suppl. 18: 45-61.

Table 1. Description of statistical sampling areas for analysis of WSR-88D Level II data in south-central Texas and northeastern Mexico in 1995 and 1996.

Location	Position Relative to the Nearest WSR-88D Radar			
			Beam Centerline[a]	
	Azimuth (deg. N)	Range (km)	Altitude (m MSL)	Statistical Sampling Area (km^2)
Rio Bravo, Tamaulipas, MX	276	75	765	5.8
Moore Air Base, Edinburg, TX	300	106	927	10.2
Lyford, TX	325	68	600	7.7
Hebbronville, TX	322	192	1,682	7.7
Bell Farm, Donna, TX	278	69	631	16.2
Seguin, TX	91	15	354	7.2
Kingsbury, TX	109	20	398	10.7

[a] At a radar elevation of 0.5 deg.

Table 2. Specifications of X-band entomological radars (10 GHz, 25KW, 1.2-deg. beam width).

ID	Operational Mode	PRF[a] (hz)	Pulse Length (μs)	Other
GBR-1	Scanning	3600	0.06	Counting annulus at 0.8 to 0.96 km range; 11 scanning elevations
GBR-2	Scanning	1700	0.25	Counting annulus at 1.21 to 1.40 km range; 8 scanning elevations
VPR	Zenith-pointing	3000	0.08	Sixty-four, 39-m altitude range intervals

[a] pulse repetition frequency

Table 3. Linear regression of mean WSR-88D reflectivity values with respect to the base-10 logarithm of the mean and beam centerline values of the aerial concentration of bollworm moth-size targets[a] measured by entomological X-band radars.

Date	Mean[b] or Centerline[c] Value	N	Linear Regression	
			S.E. (dBZ)	Adj. r^2
Jul. 1995 (GBR-2)	Mean	74	5.63	0.54[d]
	Centerline	74	5.24	0.60[d]
June 1996 (GBR-2)	Mean	91	3.71	0.20[d]
	Centerline	115	3.45	0.23[d]
Aug. 1996 (GBR-1)	Mean	93	5.57	0.59[d]
	Centerline	121	6.45	0.46[d]
Aug. 1996 (GBR-2)	Mean	20	2.78	0.89[d]
	Centerline	24	2.80	0.89[d]
Aug. 1996 (VPR)	Mean	57	4.66	0.66[d]
	Centerline	57	5.65	0.51[d]

[a] Aerial concentration of targets at the field location was derived from several elevation scans or range gates.
[b] Arithmetic mean of concentration values within the WSR-88D one-degree beam width at the field location.
[c] Concentration value at the altitude which was nearest the WSR-88D beam centerline at the field location.
[d] Significant at $\alpha = 0.05$ based on critical values of the Pearson correlation coefficient.

Table 4. Linear regression of mean WSR-88D doppler velocity values with respect to mean and beam centerline values of the radial component of wind velocity[a] measured by pilot balloons.

Date	Mean[b] or Centerline[c] Value	N	Linear Regression	
			S.E. (m/s)	Adj. r^2
Jun. 1996	Mean	43	2.4	0.61[d]
	Centerline	43	2.6	0.53[d]
Aug. 1996	Mean	24	1.7	0.71[d]
	Centerline	50	2.2	0.52[d]

[a] Radial component of wind velocity at the field location was calculated from wind velocity values interpolated at 50-m altitude intervals.
[b] Arithmetic mean of the radial wind speed values within the WSR-88D one-degree beam width at the field location.
[c] Radial wind speed value at the altitude which was nearest the WSR-88D beam centerline at the field location.
[d] Significant at $\alpha = 0.05$ based on critical values of the Pearson correlation coefficient.

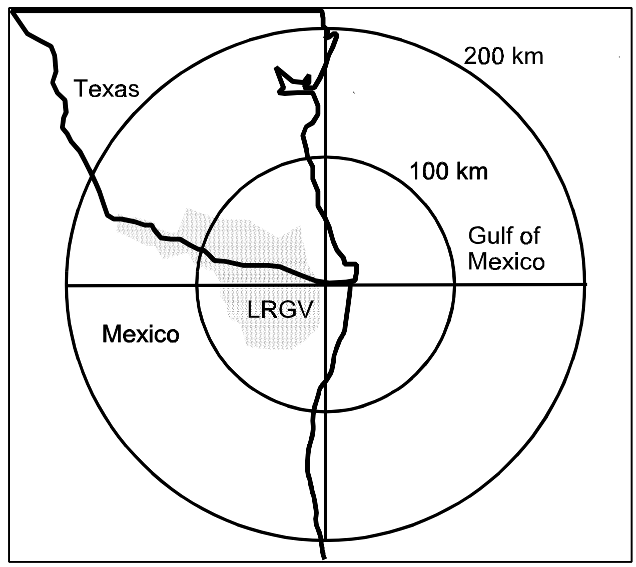

Figure 1. Map of the Brownsville WSR-88D radar coverage of the Lower Rio Grande Valley.

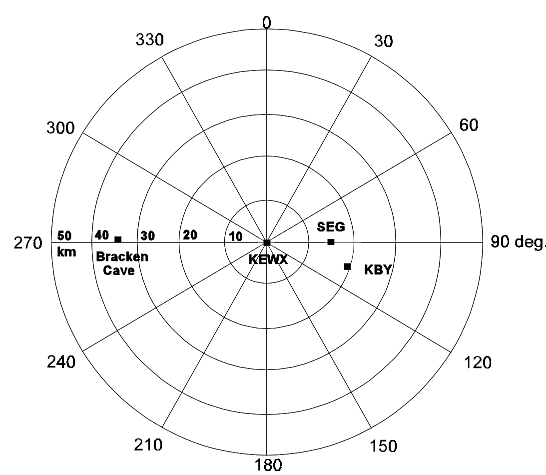

Figure 2. Map of the New Braunfels WSR-88D radar coverage of Kingsbury and Seguin, Texas.

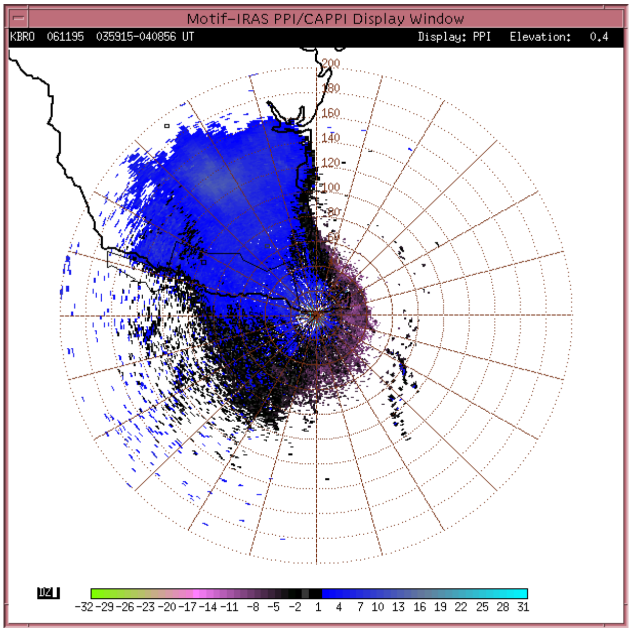

Figure 3. Brownsville WSR-88D clear-air radar reflectivity (0.4 deg. elevation scan) at 2300 h on 10 June 1995 (0400 UTC on 11 June 1995).

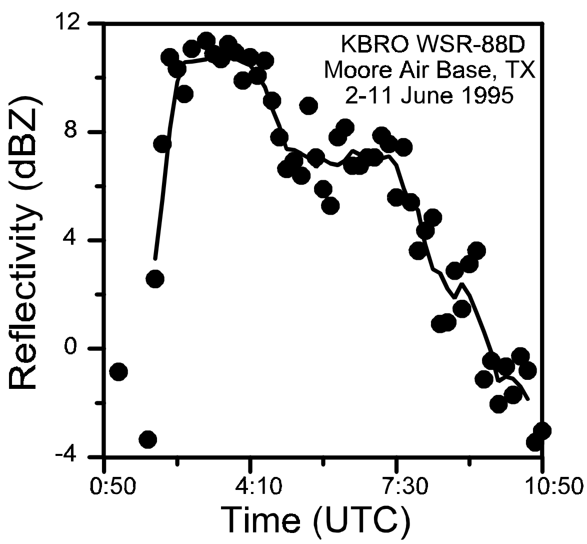

Figure 4. Nocturnal pattern of mean WSR-88D radar reflectivity (0.5 deg. elevation) at Moore Air Base, Edinburg, Texas, from 2-11 June 1995.

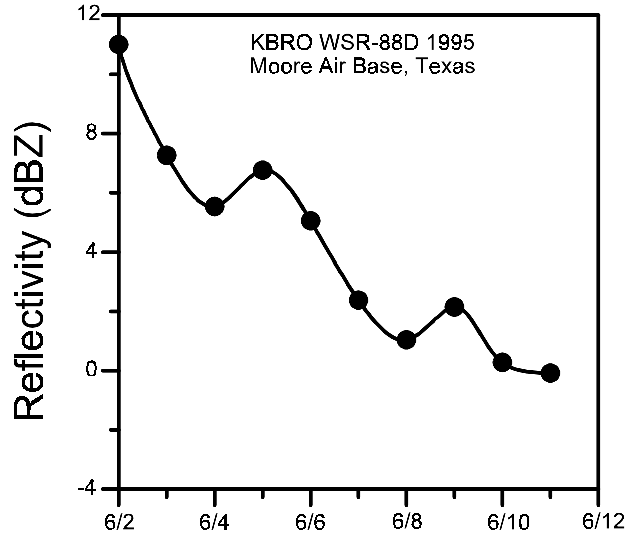

Figure 5. Mean nocturnal WSR-88D radar reflectivity (0.5 deg. elevation) at Moore Air Base, Edinburg, Texas, from 2-11 June 1995.

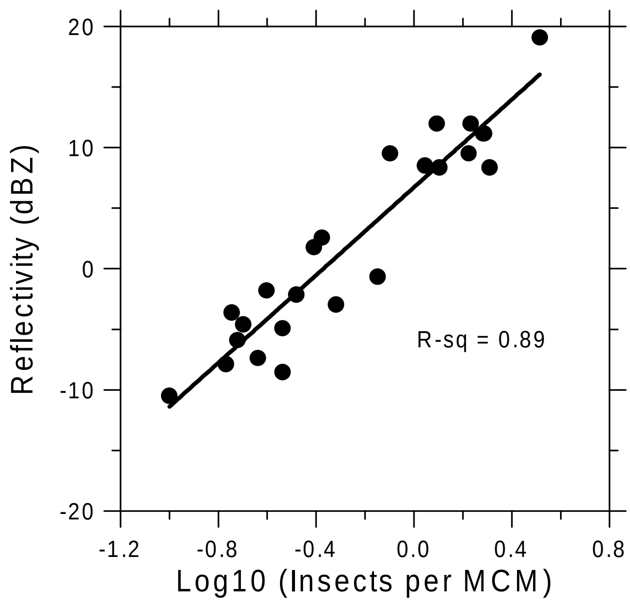

Figure 6. Scatter plot of mean WSR-88D radar reflectivity versus the log10-transform of the aerial concentration (no. per million cubic meters) of bollworm moth-size targets at Kingsbury, Texas, on 16 August 1996.

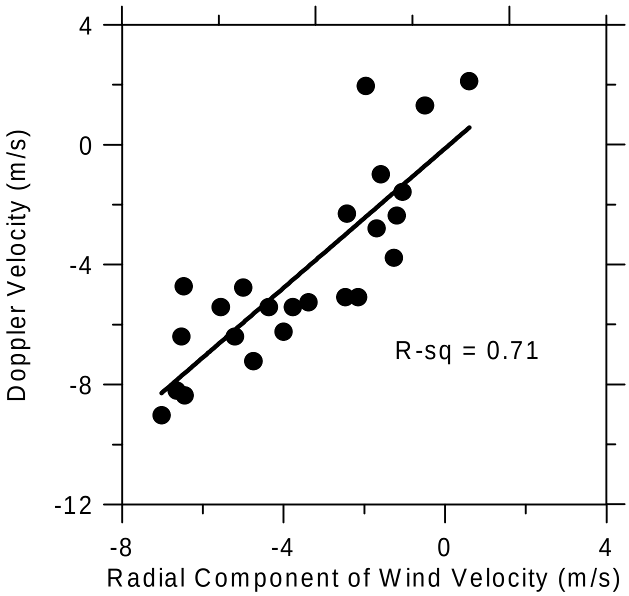

Figure 7. Scatter plot of mean WSR-88D doppler velocity versus the radial component of wind velocity at Kingsbury, Texas, on 16 August 1996.